AIMS Energy, 7(5): 539–556.
DOI: 10.3934/energy.2019.5.539
Received: 16 April 2019
Accepted: 20 August 2019
Published: 10 September 2019

http://www.aimspress.com/journal/energy

Research article

Annual performance of photovoltaic-thermal system under actual operating condition of Dire Dawa in Ethiopia

Alemayehu T. Eneyaw* and Demiss A. Amibe

School of Mechanical and Industrial Engineering, Institute of Technology, Addis Ababa University, Addis Ababa, Ethiopia

*** Correspondence:** Email: alextenaw@gmail.com; Tel: +251930603350.

Abstract: As cooling of Photovoltaic panel by water improves the electrical conversion efficiency and produces warm water as a by-product, photovoltaic thermal system is being used for cogeneration of electrical energy and hot water. In this study, the annual performance of a glazed photovoltaic thermal system (combination of PV module and solar flat plate collector) with storage tank was investigated by the dynamic computational model. The model was developed using MATLAB under actual hot water demand condition for co-generation electrical energy at Dire Dawa in Ethiopia. The computational model determines the electrical energy production and temperature of water at different points and other components of the PV-T system within a given time interval. In addition summaries of monthly and annual incident solar irradiance, electrical energy generation, thermal energy transported to storage and thermal energy supplied as hot water to end users are computed, considering the hourly hot water consumption pattern and storage size effect. The simulation, which is conducted for 20 m^2 PV-T system, consists of 12 panels with each 1.64 m^2 module areas resulted in generation 803 kWh/year thermal energy and 310 kWh/year electrical energy. The annual average electrical efficiency, thermal efficiency, hot water end use overall efficiency and co-generation (PV-T) efficiency of the system were 15.4%, 50.4%, 38%, and 65.8% respectively. The fraction of solar energy in meeting the heating load for hot water generation was 44.5% for 60 ℃ hot water supply temperature. Hence, that PV-T system can only be used for water preheating meeting at maximum half of the heating load in tropical area.

Keywords: photovoltaic thermal system; dynamic simulation; annual performance

Nomenclature: A: Area; C_p: Specific heat capacity; D_e: External diameter of tube; E: Electrical energy; fw: Collector efficiency factor; G_r: Grash of number; h: Thermal heat transfer coefficient; hf_i: Convection heat transfer of storage; I: Hourly total radiation; k: Thermal conductivity; K_T: Clearness index; l: Length; m : Mass; $\dot{m}$: Mass flow rate of water; n: Number of days in a year; N: Number of tubes; N_u: Nusselt number; $\dot{Q}_u$: Useful Heat; Ra: Rayleigh number; T: Temperature; U_l: Overall loss coefficient; V: Volume; V_{wind} : Wind Velocity; δ: Declination Angle; φ: Packing factor; $\emptyset$: Latitude angle of the location; ρ: Density; ρ_g: Ground reflection; β: Inclination angle; ϖ: Hour angle; δ: Declination Angle; η_f: Fin efficiency; η_r: Reference cell efficiency; $\alpha\tau$: Effective absorptance; σ: Stefan Boltzmann constant; β_r: Temperature coefficient

Subscripts: a : Ambient Temperature; b: Beam; c : Convection, inclined surface collector; d: Diffuse; el,a: Annual Electrical; f: Fluid; g : Glass; hws,a: Annual hot water service; i: Inlet, insulation; o: Outlet, Extraterrestrial radiation; p: Absorber Plate; P_{el}: Electrical Power; $pv-t,a$: Annual photovoltaic thermal; r: Radiation, reference; st: Storage; t: Time, thickness; th,a: Annual Thermal; w: Water; wt: Water tube

Abbreviations: DWC: Daily hot water consumption in litre; FF_{ii}: Daily hot water consumption hourly fraction; pv: Photovoltaic panel; pvt: Photovoltaic Thermal; TRNSYS: Transient systems simulation; PVsyst: Photovoltaic sizing software

1. Introduction

Due to the concern of global warming and emission of pollutants, environmental friendly energy resources such as solar energy are becoming popular. While solar energy can be directly converted into electricity by a PV module [1] hot water can be generated by converting solar energy into thermal energy by a solar collector [2]. Photovoltaic thermal (PV-T) system is a superimposition of PV panel with glazing on a flat plate solar collector to generate thermal and electrical energy simultaneously [3]. PV is considered as one of the best options for rural electrification for off-grid areas of developing countries like Ethiopia. Due to falling module unit price, might be necessary for the application of PV-T system where hot water is required in addition to electricity such as off-grid rural clinics and lodges.

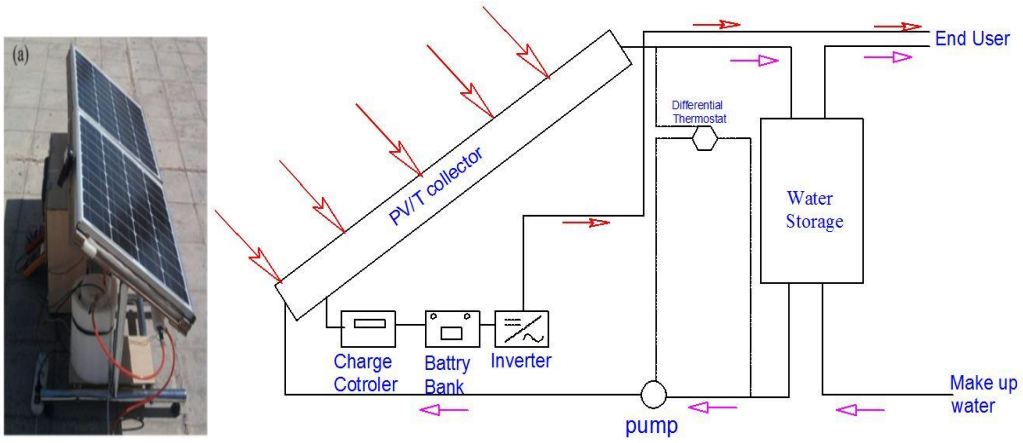

Figure 1. Experimental prototype (left) [4] and PV-T system schematic diagram (right).

A PV-T system consists of PV-T collector, balance of system (BOS) and hot water storage tank as shown in Figure 1. The PV-T collector has glazing from the top and insulation at the back. In between a superimposition of a PV-module with plate and tube absorber is placed. The PV-module converts part of the incident solar irradiance into electricity and converts most of the remaining energy into heat. Hence, heat is transferred to water in the absorber tubes increasing the water temperature and cooling the PV-module. As the water from the storage continuously circulates through the PV-T collector, the water in the storage will be heated and hot water will be continuously flow from the tank to end users.

Several researchers have investigated the performance, optimum design parameters and efficiency of PV-T system [3]. The performances of the unglazed, single glazed and double glazed PV-T systems were compared and it was concluded that the unglazed system has highest electrical efficiency and the lowest thermal efficiency [5]. Another investigation showed that the double glazed system has lowest electrical efficiency and highest thermal efficiency [6]. Hence, the single glazed PV-T can be considered as a cost-effective solution for optimum co-generation efficiency. Glazed and unglazed PV-T collectors were built and tested with water and air as working fluid, and thermal efficiency of about 58% and electrical efficiency approximately equal to 11% were obtained [7].

Effect of mass flow rate of water on performance of PV-T system was investigated and 25 kg/h was recommended as optimum value [8], while 20 kg/h was stated as optimum mass flow rate in another work [9]. These are in agreement with the range of optimum mass flow rates given in (0.001–0.0085 kg/s) [10]. The electrical, thermal and PV-T (combined) efficiencies were investigated by a dynamic model under different conditions for limited duration [11]. The performance of 1.44 kW unglazed PV-T system was investigated for different locations in Taiwan using TRNSYS software as simulation tool and electrical efficiency of 11.7–12.4% and thermal efficiency of 26.78–28.41% were obtained [12].

CFD based dynamic analysis of PV-T collectors was also carried-out by several researchers [13,14]. But these analyses were performed for limited durations due to long computational time required by multidimensional dynamic models. However, many researchers used TRNSYS software for predicting long-term performance of PV-T systems [12]. TRNSYS uses steady state or quasi-dynamic model to compute the outlet water temperature were the collector loss coefficient is considered constant, it could lead to overestimation of thermal efficiency and under estimation of electrical efficiency.

Dynamic models of PV-T system were also developed based on the solution of the transient differential equation obtained from energy balance using explicit finite difference method for time stepping[11,14]. However, most of these applications do not consider the effect of end-user hot water consumption pattern and size of the storage on hot water end-use efficiency.

The proper use of hybrid solar technology requires a tactful balance between the low-temperature requirement of the water stream to serve as a coolant, and at the same time, the high-temperature requirement for satisfying the hot water need of the end user [15]. Thus, PV-T system should be considered and designed to preheat water for a maximum of 45–50 ℃ [11].

Current researches in PV-T technology focused on increasing the overall output energy and development of this technology in terms of novel design and high performance [15]. For example, investigation of PV-T system with new configuration in Malaysia gave electrical efficiency of 13% and thermal efficiency 61%. Similarly, investigation on concentrated photovoltaic thermal collector (CPV-T) with concentration ratio of 8.5 has shown 4.7 times electrical energy output to

conventional PV-T although the electrical efficiency dropped to 8–9% due to high temperature of the PV-module [16,17]. CPV-T collectors provides incomparably greater thermal and electrical outputs compared to stand alone PV or PV-T systems as incoming solar energy is maximized inside the unit via energy-efficient concentrators [18].

In this work, the potential of conventional PV-T system shown in Figure 1 to generate electricity and preheat water using dynamic computational model based on non-linear transient differential equations. The integrated PV-T collector, storage tank and end-use system to estimate amount of thermal and electrical energy generated, considering the hourly hot water consumption pattern and storage size for tropical areas in Africa, particularly for Dire Dawa, Ethiopia.

2. Mathematical model of PV-T system

2.1. Estimation of solar irradiance on PV-T surface

The isotropic diffuse model radiation on a tilted surface, which consider three components: beam, isotropic diffuse, and solar irradiance reflected from the ground is derived as follows [19].

$$I = I_b R_b + I_d\left(\frac{1+\cos\beta}{2}\right) + I\rho_g\left(\frac{1-\cos\beta}{2}\right) \tag{1}$$

To calculate the beam and diffuse component for equation (1), a clearness index k_T shall be determined from hourly total radiation and extra-terrestrial radiation on the horizontal surface.

$$K_T = \frac{I}{I_0} \tag{2}$$

The hourly extra-terrestrial radiation on a horizontal surface for a given hour angle ϖ is given as follows.

$$I_0 = I_{sc}\left(1+0.033\cos\frac{360n}{365}\right)x\left(\cos\phi\cos\delta\sin\omega + \sin\phi\sin\delta\right) \tag{3}$$

where, the declination, (δ) is given as

$$\delta = 23.45\sin\left(360\frac{284+n}{365}\right) \tag{4}$$

The diffuse components of solar irradiance on a horizontal surface are determined from the total radiation on the horizontal surface via k_T value range with the following correlation [19].

$$\frac{I_d}{I} = \sum\begin{bmatrix} 1-0.09K_T\ for K_T \le 0.22 \\ 0.9511-0.1604K_T+4.338K_T^2-16.638K_T^3+12.336K_T^4\ for 0.22 < K_T \le 0.8 \\ 0.165\ for K_T > 0.8 \end{bmatrix} \tag{5}$$

2.2. Transient non-linear ordinary differential equations of PV-T system

For the energy balance analysis, some scientifically accepted assumptions were made for flat plate PV-T collectors. The energy analysis should start from top to bottom components, from the glass cover up to the bottom insulation. For all parts, energy balance was made considering the rate of change of energy stored in the component, energy transferred into it and leaving the component.

2.2.1. Glass cover

In analysing the glass cover, the heat transfer by radiation and convection were considered, by neglecting the conduction heat transfer within the glass. In this case, at the top of the glass heat is transferred by convection and radiation to atmospheric. On the other hand, at the bottom convection and radiation heat transfer occurs between the PV module and the glass cover. Thus, the rate of change of energy stored in the glass cover is obtained from the difference between solar irradiance absorbed by the glass plus the heat received from the PV module and the heat leaving the glass to the ambient as follows [14,20].

$$\left(m_c\right)_g \frac{\partial T_g}{\partial t} = A_{pv}\left[I_c\left(\alpha\right)_g + U_{pv-g}\left(T_{pv} - T_g\right) - U_{g-a}\left(T_g - T_a\right)\right] \tag{6}$$

2.2.2. PV module

In the PV module, heat is transferred by conduction to the absorber plate and water tubes in the backside and by natural convection and radiation to glass cover at the front side. The energy equation of the PV module is obtained by equating the variation of the stored thermal and electrical energy. In the PV module equated consider the difference between solar irradiance absorbed by the PV module, and the heat transferred from the PV module to glass and absorber, also electrical energy generated by the PV module [21].

$$\left(m_c\right)_{pv} \frac{\partial T_{pv}}{\partial t} = A_{pv} I_c \tau_g \alpha_{pv} - P_{el} - A_{pv} \frac{k_{pv}}{\delta_{pv}}\left(T_{pv} - \eta_f T_p\right) - A_{pv} U_{pv-g}\left(T_{pv} - T_g\right) - A_{pv} U_{pv-a} x\left(T_{pv} - Ta\right) \tag{7}$$

The electrical power output of the PV module is given as follows [22].

$$E = I_c \times pf \times \tau_v \eta_0 \left[1 - \varphi_c\left(T_{pv} - 25\right)\right] \tag{8}$$

2.2.3. Absorber plate

The absorber plate, which is in direct contact with the back of PV module at the top and the insulation at the back, has a function of removing heat from PV module to the water in the tubes. The rate of change of energy stored in the absorber is equated from the difference between the heat transferred to and from the absorber to the PV module. The sum of heat transferred from the absorber to the water in the tubes and to the ambient through the back of insulation, where the following

transient energy differential equation of the absorber plated is obtained [2].

$$\left(m_c\right)_p \eta_f \frac{\partial T_p}{\partial t} = \left(A_{pv} \frac{k_{pv}}{\delta_{pv}} \left(T_{pv} - \eta_f T_p\right)\right) - A_{wt} U_{p-w} \left(f_w \times T_p - \frac{T_{w,o} + T_{w,i}}{2} \right) - A_{pv} U_{i-a} \left(\eta_f T_p - T_a\right) \tag{9}$$

It shall be noted that η_f is fin efficiency of absorber plate to the tube, T_p is the maximum absorber temperature, $\eta_f T_p$ mean absorber temperature and $f_w = \left(2\eta_f - 1\right)$ is a factor that is used to determine water tube temperature from maximum absorber temperature.

2.2.4. Water stream

From energy balance for the water in the tube, the rate of change of energy stored in the water inside the tube is equal to the difference between the heat transferred from the absorber to the water in the tubes and heat transported with water from the tube to storage. As a result, the following transient differential energy equation of the water in tubes is obtained [21].

$$m_w c_w \frac{\partial T_w}{\partial t} = A_{wt} U_{p-w} \left(f_w \times T_p - \frac{T_{w,o} + Tw,i}{2} \right) - \dot{m}_w c_w \left(T_{w,o} - T_{w,i}\right) \tag{10}$$

2.2.5. Storage tank

In similar to Eq 10, the rate of change of energy stored in hot water in the tank is obtained from the difference between energy transported from the collector to the tank and energy transported with hot water to the end user plus the heat losses through the insulation of the tank as follows.

$$m_w c_w \frac{\partial T_{st}}{\partial t} = \dot{m}_w nc_w \left(T_{w,o} - T_{w,i}\right) - dhwc \frac{hf_i}{3600} c_w \left(T_{st} - Tws\right) - U_{st-a} A_{st} \left(T_{st} - T_a\right) \tag{11}$$

3. Computational model

The above transient ordinary differential equations are solved by explicit finite difference time stepping scheme. The temperature of glass, temperature of PV module, and temperature of absorber as well water outlet temperature and water storage temperature are obtained by updating the values of the current time step from the previous time step by approximating time derivatives of temperature by forwarding finite difference technique.

3.1. Glass cover

Expressing the overall heat transfer coefficient in terms of convective and irradiative components, the glass temperature at the current time step is solved as follows.

$$T_{g,i+1} = T_{g,i} + \frac{\Delta t}{m \times c_p} A_c \left(I_c \alpha_g - \left(h_{c,g-a} + h_{r,g-a}\right) \times \left(T_{g,i} - T_{a,i}\right) + \left(h_{c,pv-g} + h_{r,pv-g}\right) \times \left(T_{pv,i} - T_{g,i}\right)\right) \tag{12}$$

The radiation and convection heat transfer coefficients at the top and bottom part of the glass are given as follows [23].

$$h_{r,g-a} = \sigma\varepsilon_g \left(T_g^2 + T_a^2\right)\left(T_g + T_a\right), h_{c,g-a} = 2.8 + 3V_{wind} and, h_{r,pv-g} = \frac{\sigma\left(T_g^2 + T_{pv}^2\right)\left(T_g + T_{pv}\right)}{1/\varepsilon_{pv} + 1/\varepsilon_g - 1} \tag{13}$$

The convection heat transfer coefficient Eq 13 depends on wind velocity [24].

For the convective heat transfer between the PV module and the glass cover, the correlation of Nusselt number with Rayleigh number suggested by [14] is used.

$$N_u = 1 + 1.44\left[1 - \frac{1708\sin(1.8\beta)^{1.6}}{R_a \times \cos\beta}\right]\left[1 - \frac{1708}{R_a \times \cos\beta}\right]^{+} + \left[\left[\frac{R_a \times \cos\beta}{5830}\right]^{1/3} - 1\right]^{+} \tag{14}$$

3.2. PV module

The recursive formula for updating the PV module average temperature at the new time step is obtained as follows.

$$T_{pv,i+1} = T_{pv,i} + \frac{\Delta t}{\left(m_c\right)_{pv}} A_c\left[I - P_{el,i} - \frac{k_{pv}}{t_{pv}} \times A_{pv-p}\left(T_{pv,i} - \eta_f T_{p,i}\right)\left(h_{c,pv-g} + h_{r,pv-g}\right) \times \left(T_{pv,i} - T_{g,i}\right)\right] \tag{15}$$

3.3. Absorber plate

The maximum temperature of the new time step of the absorber plate is expressed by the following recursive formula.

$$T_{p,i+1} = T_{p,i} + \frac{\Delta t}{\eta_f\left(m_c\right)_p}\left(\frac{k_{pv}}{t_{pv}} A_{pv}\left(T_{pv,i} - \eta_f T_{p,i}\right)\right) - \frac{\Delta t}{\eta_f\left(m_c\right)_p}\left(A_{wt}U_{p-w}\left(\begin{matrix}F_w\left(2\eta_f - 1\right)T_{p,i} \\ -\frac{T_{wo,i} + Twi,i}{2}\end{matrix}\right) - U_{p-i}A_{pv}\left(\eta_f T_{p,i} - T_{a,i}\right)\right) \tag{16}$$

3.4. Water outlet

The outlet temperature of the water from the collector for the new time step is given as follows.

$$T_{wo,i+1} = T_{wo,i} + \frac{\Delta t}{\left(m_c\right)_w}\left[A_{wt}U_{p-w}\left(\left(2\eta_f - 1\right)T_p - \frac{T_{wo,i} + Twi,i}{2}\right) - \dot{m}_w c_w\left(T_{wo,i} - T_{wi,i}\right)\right] \tag{17}$$

The useful heat is evaluated as follows as per Duffie and Beckman [19].

$$Q_u = \dot{m}_w c_w\left(T_{wo} - T_{wi}\right) \tag{18}$$

3.5. Storage

The water temperature in the storage is updated at every time step as follows.

$$T_{stw,i+1} = T_{stw,i} + \frac{\Delta t}{c_w \rho_w V_{st}} \left[\dot{m}_w \, nc_w \left(T_{wi,i} - T_{wo,i}\right) - U_{st,l} A_{st} \left(T_{stw,i} - T_{a,i}\right) + \rho_w V_{st} DWC \times FF_{ii} \left(T_{stw,i} - Tws\right) \right] \quad (19)$$

3.6. Program flowchart

The developed dynamic computational model of PV-T integrated with storage was programmed in MATLAB environment. The main input to the program are the beam, diffuse irradiance and ambient temperature for the 8760 hours of the year as well as PV-T collector design parameters, location data, hot water storage and consumption pattern data are input. The incident irradiance on the PV surface is computed and determined at every hour and the useful thermal energy, glass temperature, PV temperature and absorber temperature collector outlet temperature and , hot water temperature in the storage tank and energy of hot water supplied to the end user are determined for every time step.

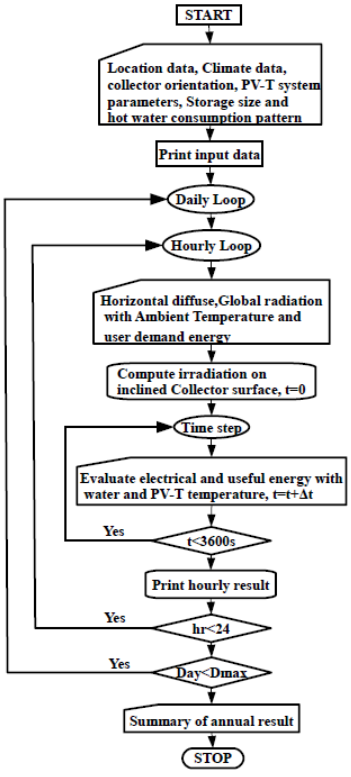

Figure 2. PV-T dynamic simulation program flowcharts.

4. Verification with the experimental result

The verification of results of the dynamic computational model of this work was done by comparison with the experimental work of similar PV-T system [4]. The input parameter of the

experimental work are given in Table 1 Using the weather data of the experimental site and PV-T parameters, simulation was conducted by the MATLAB program of dynamic computational model of PV-T system and the simulation results were compared with the experimental result for validation.

Table 1. Experimental Validation Input parameter.

Parameter	Value
Collector area	0.3
Collector fin efficiency factor	0.55
Fluid thermal capacity	4.174 kJ/kg.k
Collector Plat Absorbance	0.9
Collector loss coefficient	17 W/m^2.k
Cover Transmittance	0.95
Temperature coefficient for solar cell	0.0045
Reference Temperature for cell	25 ℃
Packing factor	1
Cell Efficiency	14%
Mass flow rate	30 kg/h

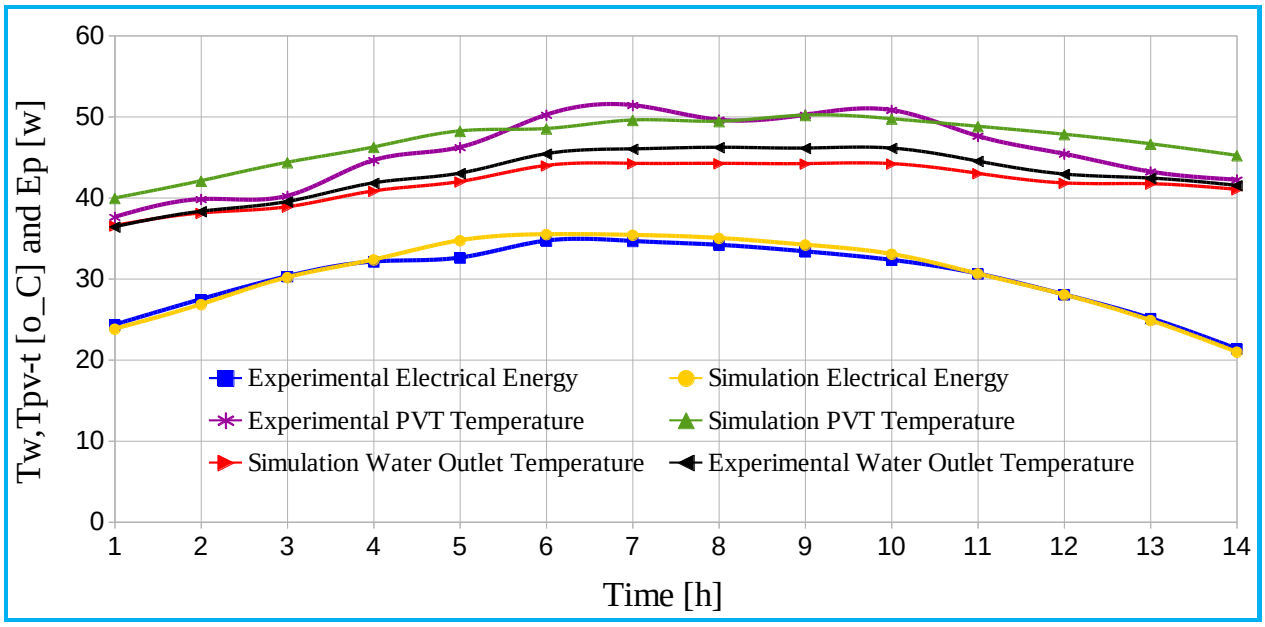

Figure 3. Comparison of the PV-T experimental and the simulation results.

Figure 3 compares the experimental and simulation results for electrical energy generation, water outlet temperature, and PV-T surface temperature. In all cases, simulation and experimental results are in good agreement with an average error of 1.77%, 2.3% and 3% for of electrical energy, water outlet, and PV-T surface temperature, respectively. The computational model has low accuracy compared to experimental investigation due to simplifications in model formation, discretization error in numerical approximation and round off error during computing. Hence, the errors are in acceptable range.

Comparison was also done with other experimental results [16,17] doing simulation using with similar solar irradiance on the collector surface and ambient temperature, and mass flow rate of water.

The result shows electrical power out-put and the PV panel temperature have similar trend with slight variation.

5. Results and discussion

Using the PV-T system simulation program, co-generation of hot water with 1 kW of electricity was investigated for an off-grid rural clinic near Dire Dawa, Ethiopia. Hourly ambient temperature and total radiation on the horizontal surface were averaged for 5 years as input to the simulation. The initial size or area of PV-T system was predicted using PVsyst, which is PV design software. As per the result of PVsyst 12 PV-T panels with each module area of 1.64 m^2 and capacity of 250 Wp are sufficient to yield an average of 1 kW during the working hours. Hence 12 PV-T collectors with a total area of 20 m^2 are interconnected for cogeneration of electric power and hot water.

5.1. Hourly Solar Irradiance incident on the collector surface

The hourly solar irradiance incident on the inclined PV-T collector was determined using Eq 1 after the clearness index was evaluated from total radiation obtained from meteorology and extra-terrestrial radiation on a horizontal surface by Eq 2 [19]. Figure 4 shows the hourly solar irradiance on the PV-T cover during the day for different months considering the geometrical orientation of the collector and location data of Dire Dawa.

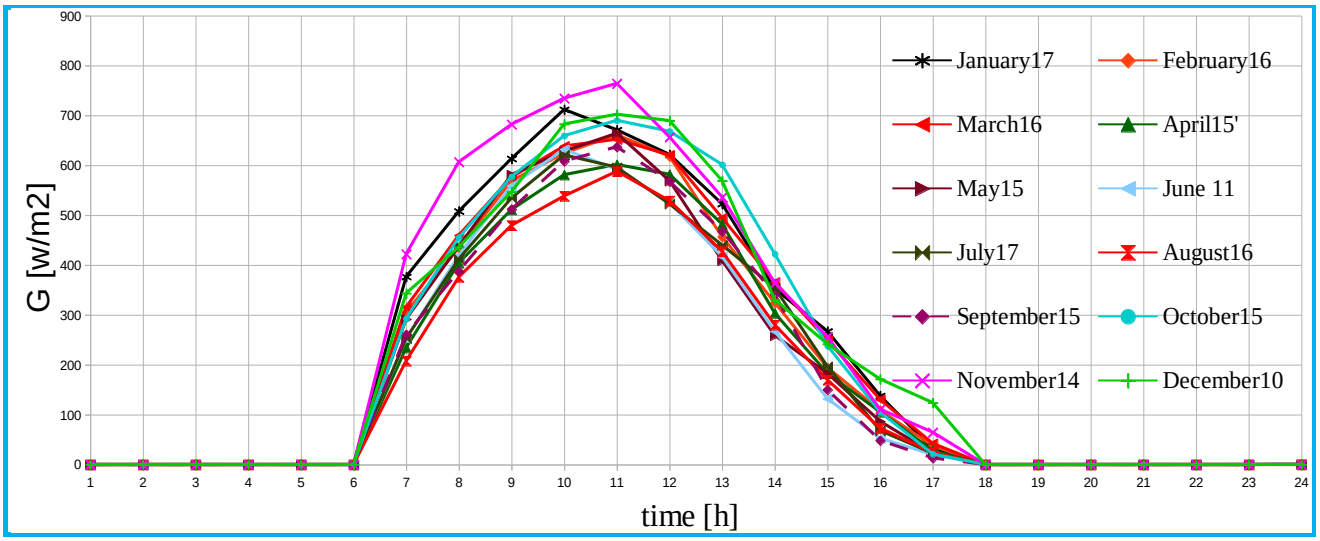

Figure 4. Solar irradiances on the collector surface for each month in W/m^2.

As shown in Figure 4, the solar irradiance reached a maximum of $780\ w/m^2$ on an average day of November and a minimum solar irradiance in August.

5.2. Glass temperature

Figure 5 shows the average hourly temperatures of the glass cover for the representative days of the months. The maximum temperature of the glass cover reached 37 ℃ in June and the minimum

temperature in February and January.

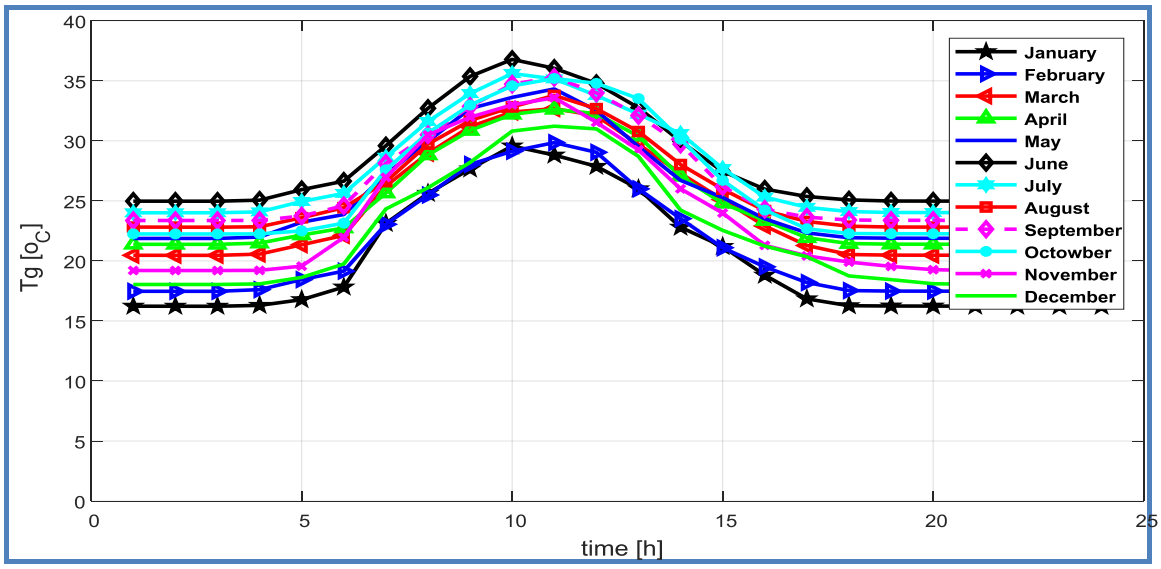

Figure 5. Glass temperatures on the representative day of the month.

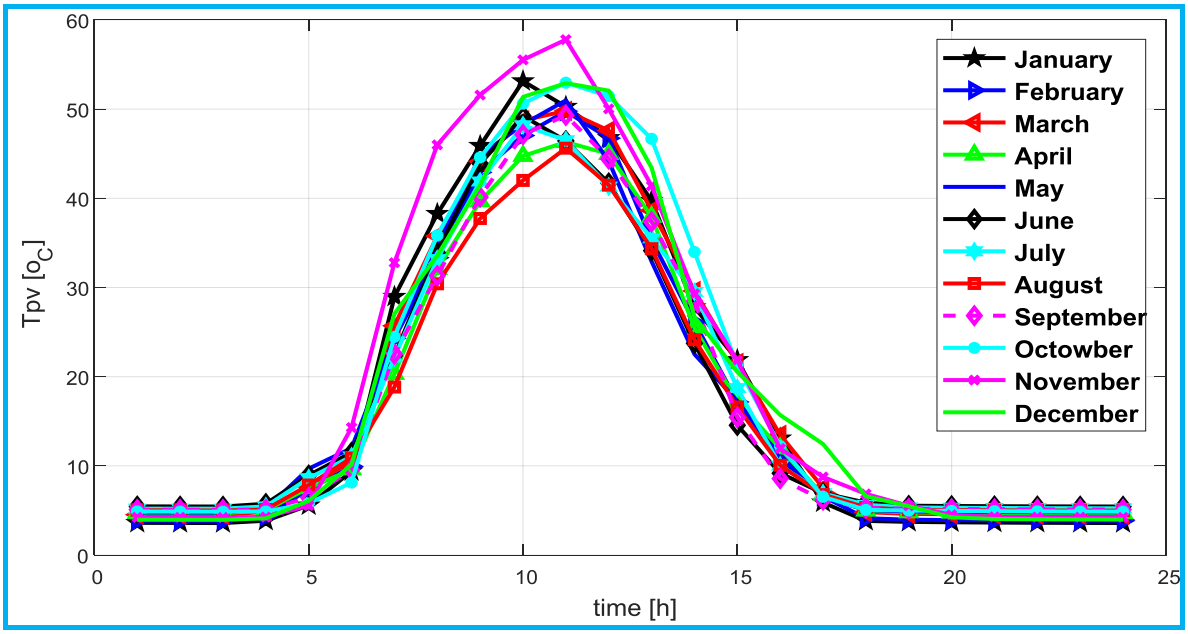

Figure 6. Photovoltaic module temperatures on representative days of the month.

5.3. Photovoltaic thermal module temperature

The PV module generates electrical energy and transfers heat to the absorber and subsequently to the water in the tubes. Figure 6 shows the maximum temperature of the PV-module, which reached 57 ℃ in November and the minimum temperature in August. The PV-module temperature is highly dependent on solar irradiance, the mass flow rate of water and many other parameters. It is possible to

decrease or increase the temperature of PV by varying these parameters. As the mass flow rate of water increases, the PV module temperature decreases. Hence optimum mass flow rate is required to keep the PV module temperature under a given value and generate hot water at the required temperature.

5.4. Electrical output

The results of annual performance simulation indicated that PV-T System simulation can generate 3720 kWh electrical energy per year, which is 10.2 kWh per day on average. This result is above the prediction of PV design software (9.22 kWh per day) for the cooling of the PV module resulted in higher PV efficiency.

5.5. Absorber temperature

Figure 7 shows the maximum temperature of the absorber plate (at the middle between tubes). The maximum hourly temperature of the absorber reached 53 ℃ in June.

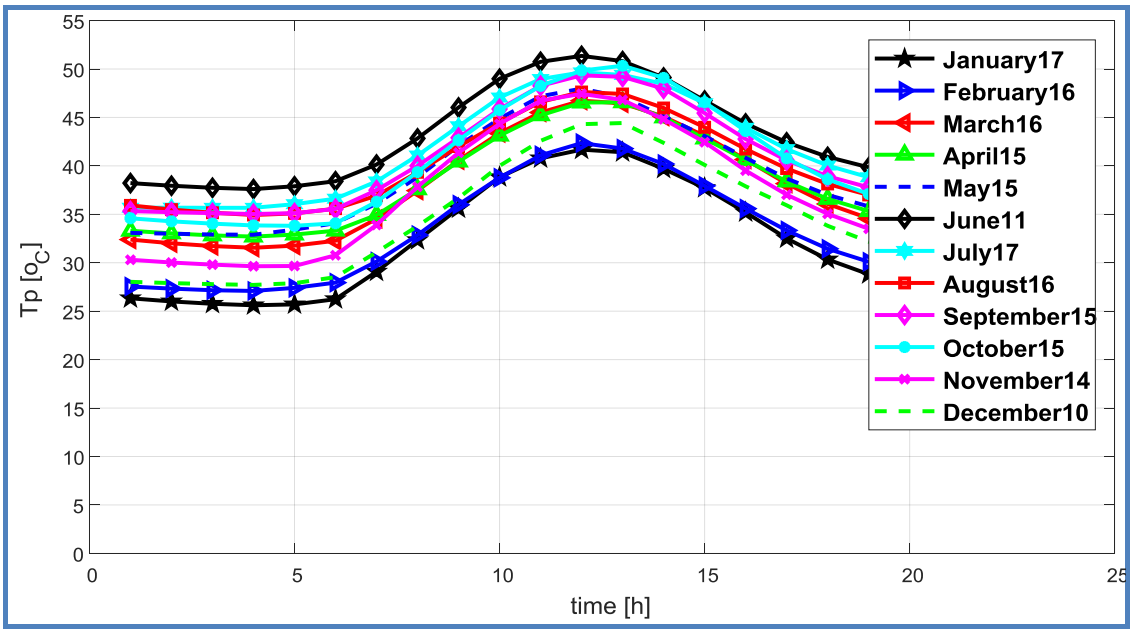

Figure 7. Maximum absorber temperature on representative days of the monthly.

5.6. The hot water outlet temperature of PV-T collector

The hot water outlet temperature from the PV-T panel depends on several parameters among which the end user hot water consumption pattern, storage tank size, and cold water supply temperature are the most important ones. Figure 8 shows the outlet temperature of PV-T collector for constant hot water consumption pattern during the working hours of a rural clinic with total daily water consumption of 0.48 m^3 per day and storage capacity of 0.48 m^3.

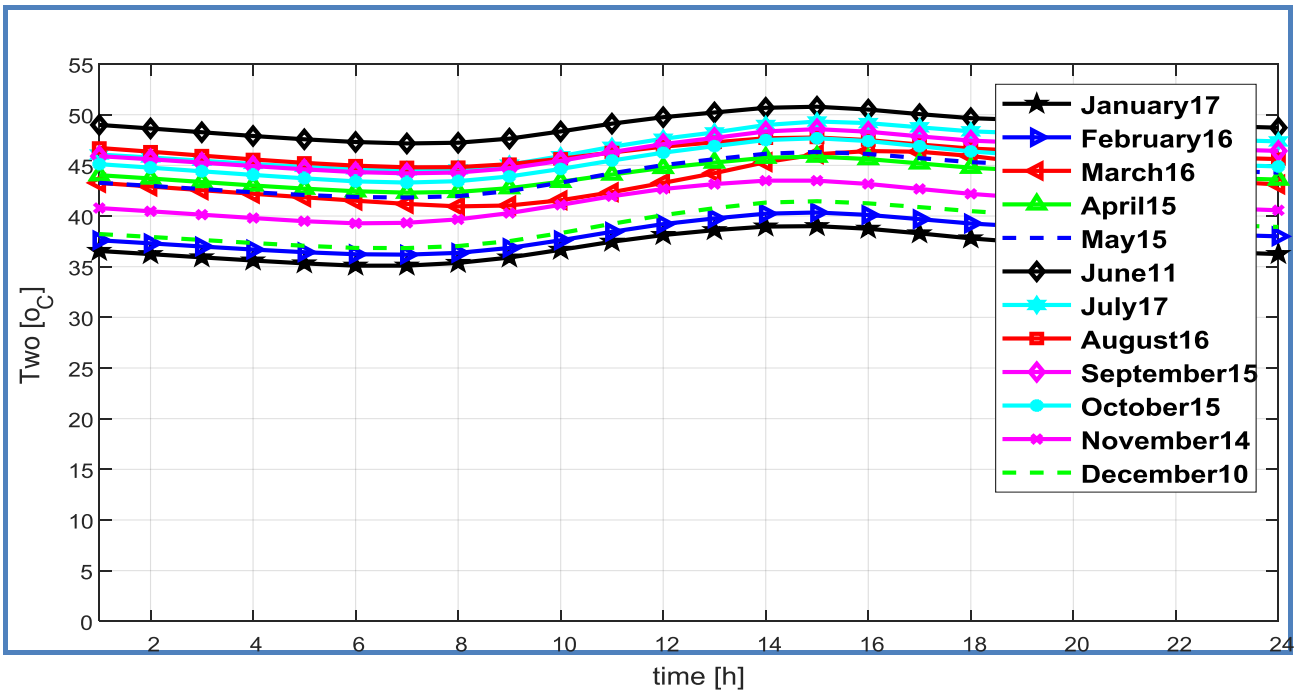

Figure 8. PV-T water outlet temperature on representative days of the month at Vs = 0.48 m^3.

The outlet temperature showed a slight increment when the storage volume is decreased. The hot water outlet temperature is highly dependent on the mass flow rate with the other parameters kept constant. Comparing circulation mass flow rate of 0.00138 kg/s per PV-T panel with 0.00164 kg/s, the PV-T water outlet temperature decreased. Table 2 shows that useful heat obtained from the collector increases slightly as the mass flow rate increases.

Table 2. Mass flow rate comparison (energy is given in kWh).

Item for comparisons	$\dot{m}_w$ = 0.00138kg/s	$\dot{m}_w$ = 0.00164kg/s [11]	Result Difference
Annual elect. energy	3684	3694	+10
Annual useful heat	10094	10621	+527
Annual sol. energy	13464	13464	0
Elec efficiency	15.4%	15.4%	0
Thermal efficiency	50.4%	50.89%	+0.49%
Hot water efficacy	37.99	37.72%	−0.27%

5.7. Hot water temperature in the storage tank

The computer program requires an input of daily hot water consumption, storage tank size, insulation thickness and an hourly fraction of daily hot water consumption, which affect the hot water temperature in the tank, is affected by besides the climate data and PV-T collector parameters. Figure 9 shows the hot water temperature in the storage tank for the case of 0.48 m^3 size tank, 0.48 m^3 daily, hot water consumption with constant hot water consumption during the working hour for a rural clinic. Sensitivity analysis of the system for different tank sizes of 0.48 m^3, 0.6 m^3 and 0.72 m^3 resulted in storage tank temperature of 43.45 ℃, 43.19 ℃, and 42.93 ℃, respectively.

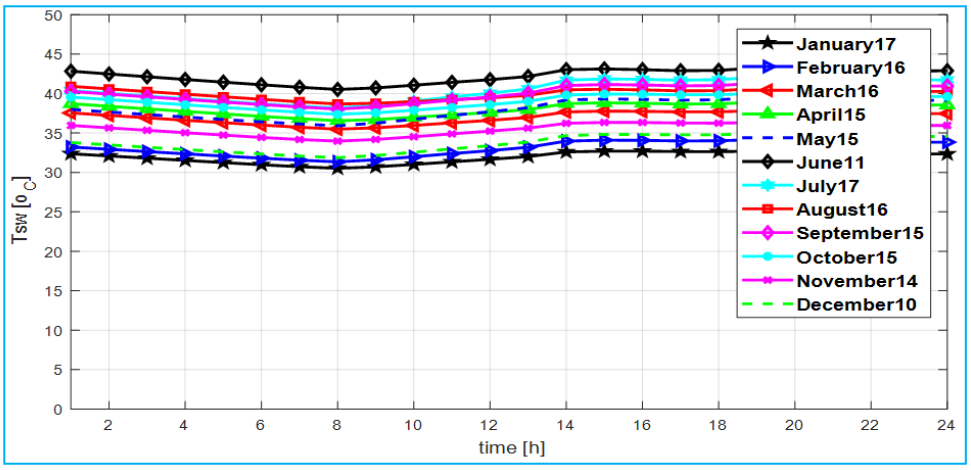

Figure 9. Water temperature in the storage tank on the representative days of the month at Vs = 0.48 m^3.

5.8. PV-T system efficiencies

PV-T generates concurrently hot water and electrical energy within one component, so it has electrical, thermal and cogeneration efficiencies. As shown in Figure 10 cogeneration efficiency (thermal plus electrical) of the system illustrated for each month of the year. The cogeneration efficiency ($\eta_0 = \eta_{th} + \eta_{ele}$) evaluates the combined output by taking the yearly total output of the system [25].

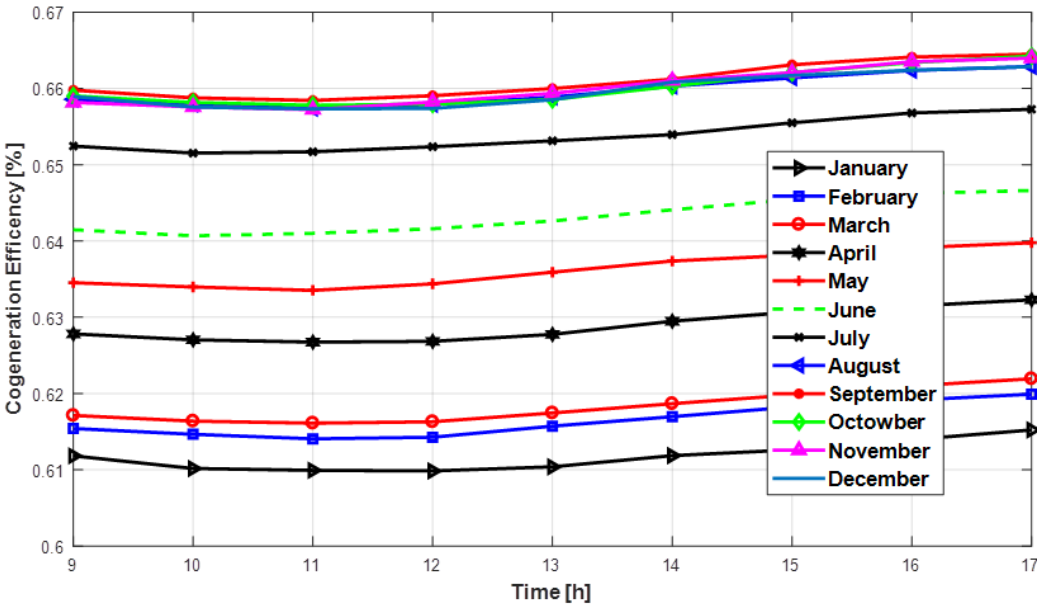

Figure 10. Cogeneration efficiency of the PVT system.

a) Electrical efficiency

$$\eta_{elc} = \frac{E_{el,a}}{G_{pv-t,a}} = 15.4\% \tag{20}$$

b) Thermal efficiency

$$\eta_{th} = \frac{Q_{th,a}}{G_{pv-t,a}} = \frac{1.012\times10^{3}}{2.007\times10^{3}}\times100 = 50.4\% \tag{21}$$

c) Hot water end use overall efficiency

$$\eta_{th,end} = \frac{Q_{hws,a}}{Q_{pv-t,a}} = 37.9\% \tag{22}$$

d) Cogeneration efficiency

$$\eta_{o} = \frac{E_{el,a} + Q_{th,a}}{G_{pv-t,a}} = 65.8\% \tag{23}$$

5.9. Comparison with selected researches of PV-T system

Table 3 shows the comparison of the other four previous works with the results of this study. While paper 1 and paper 2 gives higher thermal efficiency and slightly higher maximum water temperature, the results of these investigations are based only on one sunny day investigation moreover the hot water use pattern is neglected. Definitely, the channel type of absorber can have higher thermal efficiency compared to the tube and plate absorber considered in this study, the average thermal efficiency of paper 4 and maximum water outlet temperature is also less that of this work.

Hence, it can be concluded most of the studies conducted so far are based on the results of short term duration without considering the actual hot water storage and use pattern. Even there are few long term performance simulation results, dose not considered the effect of daily hot water use pattern by the end-user.

Table 3. Comparison of different papers.

Comparison criteria	1st paper [26] Published 2014	2nd paper [27] Published 2015	3rd paper [28] Published 2015	4th paper [29] Published 2012	5th Current research paper
Location and types of collector	Malaysia 4.2 °N,101.9 °E Glazed PV-T	Algeria 32.4 °N, 3.6 °E Glazed PV-T	Sydney 33.8 ° S,151.2 °E Both glazed and unglazed PV-T	Lyon 45.7 °N,4.8 °E Both glazed and Unglazed	Dire Dawa 9.6 °N,41.8 °E Glazed PV-T
Types of analyses	Numerical Analysis only sunny and cloudy days	Numerical and Experimental	Simulation and Validation with experimental	Simulations using TRNSYS	MATLAB Simulation with validation
Outlet water temperature of PV-T	Sunny 54 ℃ and cloudy 41 ℃ days	Not given	Max of 38 ℃ Tested for 3 days	Max 45 ℃ with axillary heater	Max 50 ℃

Continued on next page

Comparison criteria	1st paper [26] Published 2014	2nd paper [27] Published 2015	3rd paper [28] Published 2015	4th paper [29] Published 2012	5th Current research paper
Efficiencies	$\eta_{el} = 12.9\%$ $\eta_{th} = 61.3\%$ at sunny days	$\eta_{el} = 11.1\%$ $\eta_{th} = 54.5\%$ Sunny day in September	Not given	$\eta_{el} = 11\%$ $\eta_{th} = 72\%$ at zero reduced temperature	$\eta_{el} = 15.4\%$ $\eta_{th} = 50.4\%$ Annual efficiency
Daily hot water Consumption Pattern	Not considered	Not considered	Not considered	Not considered as variable	Considered
Mass flow rate	No specified	No specified	0.217 kg/s m^2	0.0125 kg/s m^2	0.0013 kg/s
Hot water Storage	Heat up in one day	No description	Yes Temperature of storage is set equal to that of main water every morning	Yes	Yes Storage temp. at every morning is obtained from previous day

Note: The reduced temperature corresponds to the difference between the fluid mean temperature and the ambient temperature , divided by the solar radiation [29].

6. Conclusions

A dynamic computational model of a PV-T system integrated with storage tank and hot water end use was developed and the accuracy of the computer program was checked by comparing the model with experimental results. Simulation result of cogeneration of electricity and hot water for rural clinic around Dire Dawa was investigated. The results indicated that a PV-T system can supply hot water up to a maximum of 45 ℃, attaining the following achievements PV efficiency of 15.4%, thermal efficiency of 50.4%, hot water end uses overall efficiency of 37.9% and cogeneration efficiency of 65.8%. The fraction of PV-T system in meeting the hot water energy demand was 44.5% when the hot water supply temperature is 60 ℃. There is about more than 10% difference between the thermal efficiency and overall end-use efficiency of hot water generation due to the time shift between generation and consumption of hot water.

The research indicated that PV-T system has good PV and cogeneration efficiencies. The effect of considering daily hot water demand fraction variability and storage size effect resulted in hot water end use overall efficiency close to the reality and a maximum hot water supply temperature becomes below 45 ℃. Hence, a PV-T system can be used only as a preheater for hot water generation systems even in tropical African areas meeting at maximum up to 50% of the energy demand. Moreover, the time shift between hot water generation and consumption as well as dilution of hot water by cold make-up water causes degradation of thermal energy and lower end-use efficiency and hot water temperature.

Conflict of interest

The authors declare no conflict of interest.

References

1. Messenger RA, Ventre J (2005) *Photovoltaic Engineering Systems.* Second edition Taylor & Francis e-Library.
2. Bekele A, Alemu D, Mishra M (2011) Large-scale solar water heating systems analysis in Ethiopia: A case study. *Int J Sustainable Energy* 32: 1–22.
3. Zondag HA (2008) Flat-plate PV-Thermal collectors and systems: A review. *Renewable Sustainable Energy Rev* 12: 891–959.
4. Sardarabadi M, Fard MP, Sardarabadi H, et al. (2012) Computer modelling and experimental validation of a photovoltaic thermal (PV/T) water based collector system. *2nd International Conference on Power and Energy Systems (ICPES2012)* 56: 75–79.
5. Abdelrazik AS, Al-sulaiman FA, Saidur R, et al. (2018) A review on recent development for the design and packaging of hybrid photovoltaic/thermal (PV/T) solar systems design of PV. *Renewable Sustainable Energy Rev* 95: 110–129.
6. Kazemian A, Hosseinzadeh M, Sardarabadi M, et al. (2018) Effect of glass cover and working fluid on the performance of photovoltaic thermal (PVT) system : An experimental study. *Solar Energy* 173: 1002–1010.
7. Marc-Alain Mutombo N, Inambao F, Bright G (2016) Performance analysis of thermosyphon hybrid photovoltaic thermal collector. *J Energy South Afr*, 27: 28–38.
8. Kalogirou SA (2001) Use of TRNSYS for modelling and simulation of a hybrid pv-thermal solar system for Cyprus. *Renewable Energy* 23: 247–260.
9. Yal çin L, Öztürk R (2013) Performance comparison of c-Si, mc-Si and a-Si thin film PV by PVsyst simulation. *J Optoelectron Adv Mater* 15: 326–334.
10. Chow TT (2010) A review on photovoltaic/thermal hybrid solar technology. *Appl Energy* 87: 365–379.
11. Chow TT (2003) Performance analysis of photovoltaic-thermal collector by explicit dynamic model. *Sol Energy* 75: 143–152.
12. Huang CY, Huang CJ (2014) A study of photovoltaic thermal (PV/T) hybrid system with computer modeling. *Int J Smart Grid Clean Energy* 3: 75–79.
13. Pauly L, Rekha L, Vazhappilly CV, et al. (2016) Numerical simulation for solar hybrid photovoltaic thermal air collector. *Procedia Technol* 24: 513–522.
14. Bhattarai S, Oh JH, Euh SH, et al. (2012) Simulation and model validation of sheet and tube type photovoltaic thermal solar system and conventional solar collecting system in transient states. *Sol Energy Mater Sol Cells* 103: 184–193.
15. Sultan SM, Efzan MNE (2018) Review on recent photovoltaic/thermal (PV/T) technology advances and applications. *Sol Energy* 173: 939–954.
16. Du B, Hu E, Kolhe M (2012) Performance analysis of water cooled concentrated photovoltaic (CPV) system. *Renewable Sustainable Energy Rev* 16: 6732–6736.
17. Kolhe M, Bin D, Hu E (2012) Water cooled concentrated photovoltaic system. *Int J Smart Grid Clean Energy* 2–6.
18. Daneshazarian R, Cuce E, Cuce PM, et al. (2018) Concentrating photovoltaic thermal (CPVT) collectors and systems : Theory, performance assessment and applications. *Renewable Sustainable Energy Rev* 81: 473–492.

19. Duffie JA, Beckman WA, Worek WM (2003) *Solar Engineering of Thermal Processes, 4nd Eds*, 116.
20. Chow TT, He W, Ji J, et al. (2007) Performance evaluation of photovoltaic–thermosyphon system for subtropical climate application. *Sol Energy* 81: 123–130.
21. Ammar MB, Chaabene M (2009) A dynamic model of hybrid photovoltaic/thermal panel. *Int Renewable Energy Congress* 19–24.
22. Guarracino I, Mellor A, Ekins-daukes NJ, et al. (2016) Dynamic coupled thermal-and-electrical modelling of sheet-and-tube hybrid photovoltaic/thermal (PVT) collectors. *Appl Therm Eng* 101: 778–795.
23. Hossain MS, Pandey AK, Selvaraj J, et al. (2019) Thermal performance analysis of parallel serpentine flow based photovoltaic/thermal (PV/T) system under composite climate of Malaysia. *Appl Therm Eng* 153: 861–871.
24. Baxter R, Hastings N, Law A, et al. (2008) Fundamentals of heat and mass transfer. 39.
25. Al-Waeli AHA, Sopian K, Kazem HA, et al. (2017) Photovoltaic/Thermal (PV/T) systems : Status and future prospects. *Renewable Sustainable Energy Rev* 77: 109–130.
26. Sultan SM, Fadhel MI, Alkaff SA (2014) Performance analysis of the photovoltaic/thermal collector (PV/T) system for different Malaysian climatic conditions. *Appl Mech Mater* 467: 522–527.
27. Hocine HBC, Touafek K, Kerrour F, et al. (2015) Model validation of an empirical photovoltaic thermal (PV/T) collector. *Energy Procedia* 74: 1090–1099.
28. Bilbao JI, Sproul AB (2015) ScienceDirect detailed PVT-water model for transient analysis using RC networks. *Sol Energy* 115: 680–693.
29. Dupeyrat P, Ménézo C, Fortuin S (2014) Study of the thermal and electrical performances of PVT solar hot water system. *Energy Build* 68: 751–755.